INFLUENCE OF INTERNAL GEOMETRY UPON REGENERATIVE PUMP PERFORMANCE

by

Steven C. Mason

Submitted in partial fulfillment of the requirements for the Degree of Bachelor of Science in Mechanical Engineering

at the

Massachusetts Institute of Technology

May 1957

Signature of Author _____ May 29, 1957

Certified by _____ Thesis Adviser

Accepted by _____ Chairman, Departmental Committee of Undergraduate Thesis

ABSTRACT

INFLUENCE OF INTERNAL GEOMETRY UPON REGENERATIVE PUMP PERFORMANCE

by

Steven C. Mason

Submitted to the Department of Mechanical Engineering on May 20, 1957, in partial fulfillment of the requirements for the Degree of Bachelor of Science.

An experimental investigation of a regenerative pump was performed with two channel diameters (2 inches and 1.25 inches) - each with 40 and 20 blades in the pump impeller. The experimental performance characteristics were compared with a theoretical analysis of the fluid mechanism of regenerative pumps. The theoretical analysis involves the selection of two empirical parameters and it was hoped that a simple relation between the circulatory flow coefficient and the local geometry of the channel could be discovered as a result of this project. The results of this investigation show that there is no immediately obvious relation between K_c and local geometry and a value for the circulatory flow coefficient is best found by using a trial and error approach.

Thesis Supervisor - W. A. Wilson

Title - Professor of Mechanical Engineering

LIST OF SYMBOLS

P	pressure
H	head in ft. of fluid pumped
Q	volume rate of flow
W	power input to the pump
K_c	circulatory flow coefficient
g	acceleration of gravity
u	internal energy at any point
V	velocity of fluid
U	wheel speed
Z	number of blades in the impeller

Dimensions of Pump

r	radius
R	radius of open channel
r_g	radius to the centroid of the cross section of the channel
r_i	radius to the mean streamline entering the impeller passage
r_o	radius to the mean streamline leaving the impeller passage
b_i	radial length of the circulatory flow area entering the impeller
b_o	radial length of the circulatory flow area leaving the impeller
A	cross sectional area of the pump channel
D	diameter to the cg of the channel

Greek Symbols

ρ	density of fluid pumped
ω	angular velocity of the impeller, radians/sec.
θ_P	angular measurement over which the input power is distributed
θ_H	angular measurement of the linear region of the pump, radians
τ	torque input to the pump
α	V_{ti}/U_i
σ	V_{to}/U_o

Dimensionless Performance Symbols

ψ	Q/Q_s, ratio of actual flow to solid body rotation of the channel area
$\frac{d\psi}{d\theta}$	$\frac{gH}{\rho\omega^2 D^2}\frac{1}{\theta_P}$, pressure coefficient
η	$\frac{\rho QH}{W}$, efficiency

Subscripts

c	circulatory flow
s	solid body rotation
t	tangential direction
o	open channel
i	impeller

LIST OF ILLUSTRATIONS

FORWARD

This investigation is a continuation of a research program at the Massachusetts Institute of Technology which was started in September, 1952. At that time, a grant-in-aid was established by the Worthington Corporation for the purpose of conducting an investigation of the regenerative pump.

The initial step of the research program was to establish a theory which would predict the internal performance of the regenerative pump design. This theory was applied to data from commercial pumps, a large lucite experimental model *(2), and a smaller cast steel experimental design (1). The results of these experiments lead to the present investigation.

The author would like to acknowledge the support and assistance of Professor W. A. Wilson and D. P. DeWitt.

Note: *() refers to Bibliography

TABLE OF CONTENTS

INTRODUCTION

The performance characteristics of the hydrodynamic unit which is called a regenerative pump show an inverse relation of head and power to capacity. The efficiency of the regenerative pump design is not very impressive, but it is comparable with the efficiencies of other pump designs of similar specific speeds. The regenerative pump has several industrial application because of its performance characteristics and low specific speeds: ex. lubrication, filtering and control systems.

There are several internal designs for commercial regenerative pumps. One of the common designs is the "inverted L" channel which is shown in Figure A. The design which was the subject of this investigation is the "half-torus" channel (Figure B) that was developed for experimental work.

The vanes or blades in the experimental unit are cast into the face of the impeller. The fluid passes through the open channel and circulates repeatedly through the vanes. The increase of angular momentum of the fluid that is in the centrifugal field of the impeller is dissipated in the channel and causes the tangential pressure gradient within the pump. The regenerative pump is very appropriately named because of the internal circulatory flow which has a regenerative action.

I CIRCULATORY FLOW THEORY

The theoretical expressions for the performance characteristics of the regenerative pump were first postulated by Wilson, Santalo and Oelrich (3). These expressions could not be applied directly to the geometry of the present experimental design and were modified by DeWitt (1). The modified expressions were re-derived by the author and applied to the present investigation.

I-a Areas of Operation

Within the regenerative pump, there are three distinct areas of operation:

1. The inlet and acceleration region extends from the inlet to a point between taps 1 and 2 (see Figure D for location of the pressure taps.)
2. The linear region of operation extends from tap 2 to tap 7 and is the region for which the theoretical expressions are derived.
3. The outlet and deceleration region of operation extends from tap 7 to the outlet.

I-b Derivation of Theoretical Performance Expressions

I-b-1 Assumptions:

A hypothetical model was developed to facilitate the derivation of the theoretical expressions for pump operation. This model is applicable only to the linear

region of the pump and incorporates the following assumptions:

1. Flow is considered to be steady in time.
2. Flow is incompressible.
3. All processes within the pump are adiabatic.
4. The tangential pressure gradient is constant throughout the linear region and is independent of radius.
5. Impeller flow areas are equal; i.e. area of circulatory flow entering the impeller equals the circulatory flow area leaving the impeller.

I-b-2 Definitions

Two terms are introduced to simplify the derivation.

1. The through flow is defined as

$$Q = \int_A V_t \, dA$$

where A is equal to the cross-sectional area of the open channel.

2. The circulatory flow is called Q_c and is associated with the circulatory velocity component - V_c .

I-b-3 Control Volumes

In view of assumption 4, the analysis of any meridional section of the fluid in the impeller and the channel will yield theoretical performance expressions for pump operation in the linear region. Two control volumes were isolated - a differential element, $d\theta$, of the fluid in the channel and a similar element of the fluid in the impeller (Figure E) - and the steady flow energy equations and momentum

relations were applied to each.

The following is a summary of the results of the analysis. (For detailed analysis see DeWitt (1).)

The consideration of the impeller control volume as shown in Figure E yields:

$$\frac{dW}{d\theta} = \omega \rho Q_c (\sigma U_o r_o - \alpha U_i r_i) + \frac{dP}{d\theta} r_g A \omega \qquad (1)$$

by angular momentum

$$\frac{P_o - P_i}{\rho} = \frac{\alpha^2 U_i^2 - \sigma^2 U_o^2}{2} + \sigma U_o^2 - \alpha U_i^2 - g H_{ci} \qquad (2)$$

by steady flow

where $\sigma = \frac{V_t \text{ actual}}{U_o}$

$\alpha = \frac{V_t \text{ actual}}{U_i}$

$g H_{ci}$ circulatory losses in the impeller.

The application of the same relations to the channel control volume give:

$$\frac{dP}{d\theta} = \frac{\rho Q_c}{r_g A} (\sigma U_o r_o - \alpha U_i r_i) - g H_t \qquad (3)$$

by angular momentum

$$\frac{P_o - P_i}{\rho} = \frac{\alpha^2 U_i^2 - \sigma^2 U_o^2}{2} + \frac{\omega Q}{r_g A} (\sigma r_o^2 - \alpha r_i^2) + g H_{cc} \qquad (4)$$

by steady flow

where $g H_{cc}$ circulatory flow losses in the channel area

$g H_t$ tangential flow losses in the channel

Expressions 2 and 4 can be equated because they are both expressions for the radial pressure rise in the two control volumes between the same two points. This yields a theoretical expression for the head losses due to circulatory flow.

$$g H_c = g H_{cc} + g H_{ci} = (\sigma U_o^2 - \alpha U_i^2)\left(1 - \frac{Q}{Q_s}\right)$$

I-b-4 Assumed Circulatory Flow Losses

The circulatory flow loss is considered to be comprised of two terms:

a) Friction and turbulent losses are encountered due to shear stresses at the walls and the nature of the flow. Wilson (3) suggests that this loss is proportional to the circulatory flow velocity squared.

$$\text{friction losses} = K_c \left(\frac{Q_c}{r_i b_i}\right)^2$$

b) Blade entrance losses are encountered due to the sudden acceleration of the fluid as it passes from the low velocity channel flow to the high velocity impeller region. Spannhacke suggests that this loss is in the form of a kinetic energy term.

$$\text{blade entrance losses} = \frac{(1-\alpha) U_i^2}{2} + K_c \left(\frac{Q_c}{r_i b_i}\right)^2$$

The sum of these two losses is the total circulatory flow loss - $g H_c$

$$g H_c = \frac{(1-\alpha) U_i^2}{2} + K_c \left(\frac{Q_c}{r_i b_i}\right)^2 \qquad (5)$$

I-b-5 Performance Expressions

A theoretical expression for Q_c is obtained by equating the assumed circulatory losses to the theoretical losses.

$$Q_c = \frac{r_i b_i}{\sqrt{K_c}} \left[\overbrace{(\sigma U_o^2 - \alpha U_i^2)\left(1 - \frac{Q}{r_g A}\right) - \frac{(1-\alpha)^2 U_i^2}{2}}^{X} \right]^{\frac{1}{2}} \quad (6)$$

This expression for Q_c is substituted into equation 3 to yield a theoretical pressure gradient which will be compared with experimental results.

$$\frac{dP}{d\theta} = \frac{\rho r_i b_i}{r_g A} \sqrt{\frac{1}{K_c}} \left[\sigma U_o r_o - \alpha U_i r_i \right] [\ X\ ]^{\frac{1}{2}} \quad (7)$$

The through flow, Q, must also be evaluated theoretically. Previous experimental work has shown that a reasonable assumption was a linear velocity gradient throughout the channel. This yields:

$$Q = \int_A V_t \, dA = \left[\frac{\sigma U_o + \alpha U_i}{2} \right] A \quad (8)$$

The expression for Q_c and the pressure coefficient were non-dimensionalized for ease in calculations. This form is given in the Appendix.

II DESCRIPTION OF APPARATUS AND TEST PROCEDURE

II-a Description of the Pump

The pump is shown schematically in Figure C. The back support plate and the cover are made of steel and the surface between the two is machined so that a close fit can be achieved to minimize any leakage through the joint. A

two inch diameter, half torus channel is machined into the inside of the cover to act as the open passage. Inlet and outlet ports are cut through the cover and are separated by a Plaster of Paris stripper. (Figure D)

The impeller is also machined from steel with a brittle, low melting point alloy insert into which the impeller channel and 40 blades are cast. Four radial seals are machined upon the edge of the impeller to form a clearance of 0.008 inches between the impeller and the cover. The clearance between the impeller face and the front cover was held at approximately 0.005 inches throughout the experimental work to minimize any leakage across the stripper.

II-b Instrumentation

The flow through the pump was controlled by a gate valve at the outlet and was measured by a venturi tube at the inlet. The venturi was connected to an inclined manometer to determine the pressure at the venturi throat.

The pressure rise within the pump was measured by static pressure taps along the channel which were connected to a water manometer.

A cradled dynamometer, rated at 2.62 in. -# of torque, was used to furnish the input power to the impeller and the torque was measured by a sliding weight. The speed of the motor was measured by a commercial strobatac and was held constant by the use of a Veriac throughout each test.

III RESULTS OF EXPERIMENTAL WORK

The results of the experimental work are presented in Graphs 1, 2, 3, and 4. Graph 1 shows the performance characteristics of the pump with 40 blades in the impeller and a channel radius of 1 inch. The radius of the channel was then held constant (1 inch) and every other blade was removed. Graph 2 illustrates the performance characteristics of the pump with 20 blades in the impeller and with a channel radius of 1 inch. The open channel and the impeller passage were then filled with Plaster of Paris to a passage radius of 0.625 inches and tests were made for 40 blades in the impeller (Graph 3) and 20 impeller blades. (Graph 4)

In each of the experimental runs, the head coefficient and power coefficient are plotted against φ_E ($\varphi_E = \frac{Q+Q_L}{Q_s}$) φ_E is based upon the flow which was measured at the pump inlet by the venturi. This measured flow includes the pump through-flow plus the leakage flow across the stripper. DeWitt's (1) leakage analysis (See Appendix) was then applied to the experimental curves to correct the value of φ_E by eliminating the leakage flow (φ_L) and curves for each geometry were calculated (Graphs 5, 6, 7, and 8) based upon the delivered flow to the pump outlet.

The experimental performance curves exhibit several characteristics which are of interest. When the radius of the channel is maintained at a constant value of either 1 inch or 0.625 inches and the number of blades in the impeller is

changed from 40 to 20, the pressure coefficient is increased at low values of φ_E . Above a value of φ_E of approximately 0.4, the pressure coefficient is less for the case of a reduced number of blades. The maximum internal efficiency (which is based upon the measured inlet flow, i.e. $Q + Q_L$) also decreases with a decrease in the number of impeller blades and occurs at a lower value of φ_E .

If the number of blades in the impeller is maintained at either 40 or 20 while the channel radius is decreased, the pressure coefficient is increased at low values of φ_E and decreases for φ_E above 0.6. The maximum efficiency is also decreased and occurs at a lower value of φ_E for the case of reduced number of blades.

When both the channel radius and the number of blades are decreased, the pressure coefficient increases while the maximum efficiency decreases. The specific speed of the pump also decreases for this case. Another characteristic of the geometric change from $R = 1$ inch to $R = 0.625$ inches and $Z = 40$ to $Z = 20$ is that the shape of the pressure coefficient curve changes. (Graphs 1 and 4). This is inherent in the theoretical analysis as evidenced by the match between the theory and experimental curves as shown in Graphs 9 and 12.

IV COMPARISON BETWEEN THEORY AND EXPERIMENTAL RESULTS

The match between the theoretical and experimental pressure coefficients for each of the configurations tested is shown in Graphs 9, 10, 11, and 12. The dashed curves are the

result of introducing empirically evaluated performance parameters (σ and K_c) into the non-dimensionalized theoretical expression for the pressure coefficient (See Appendix for this expression). The procedure for establishing a correlation between the theoretical predictions and the experimental results involved the following steps:

a. The measured experimental flow rate was increased by a small amount to account for the flow leakage across the impeller seals. The details of the leakage correction are shown in the Appendix and the results of correcting the flow through the pump are shown in Graphs 5, 6, 7, and 8.

b. The values for r_i and r_o were determined upon the basis of equal circulatory flow areas entering and leaving the impeller.

c. A value of σ was tentatively selected in accordance with Busemann's work. (3)

d. A match between the theoretical and experimental curves was forced at $\varphi = .5$. This was accomplished by substituting the experimental head coefficient at $\varphi = .5$ into the theoretical expression using a value of σ determined in (c). This permits the evaluation of K_c .

e. Using the values of σ and K_c determined above, the entire theoretical performance curve was calculated and compared with the test data.

The process was repeated until a reasonable match was obtained for each pump configuration tested.

The value of σ which appeared to give a reasonable match between the theoretical analysis and the experimental follows Busemann's (3) work. As the number of blades decreases, σ also decreases. The value of σ is also seen to be a function of the radius ratio (r_i/r_o). As this ratio approaches 1, σ approaches 0.

V CONCLUSIONS

The relations between σ and the number of blades and channel geometry as stated in previous works has been reconfirmed.

One of the objects of this investigation was to experiment upon several pump configurations with the hope of finding a simple relationship between the circulatory flow coefficient, K_c, and local pump geometry. A study of the values of K_c which give a reasonable match between the theory and experimental work, show that there is no obvious relation between K_c and local geometry. The best method for determining a suitable value of this parameter for any configuration still appears to be a forced fit such as was used in the preceding analysis.

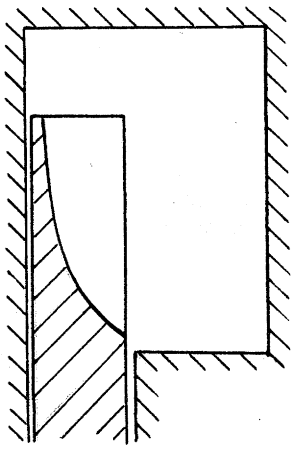

"INVERTED L" CHANNEL
COMMERCIAL DESIGN

FIGURE A

"½ TORUS" CHANNEL
EXPERIMENTAL DESIGN

FIGURE B

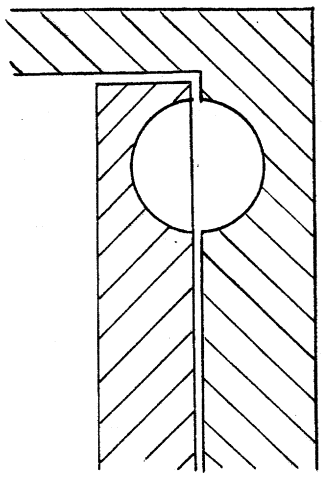

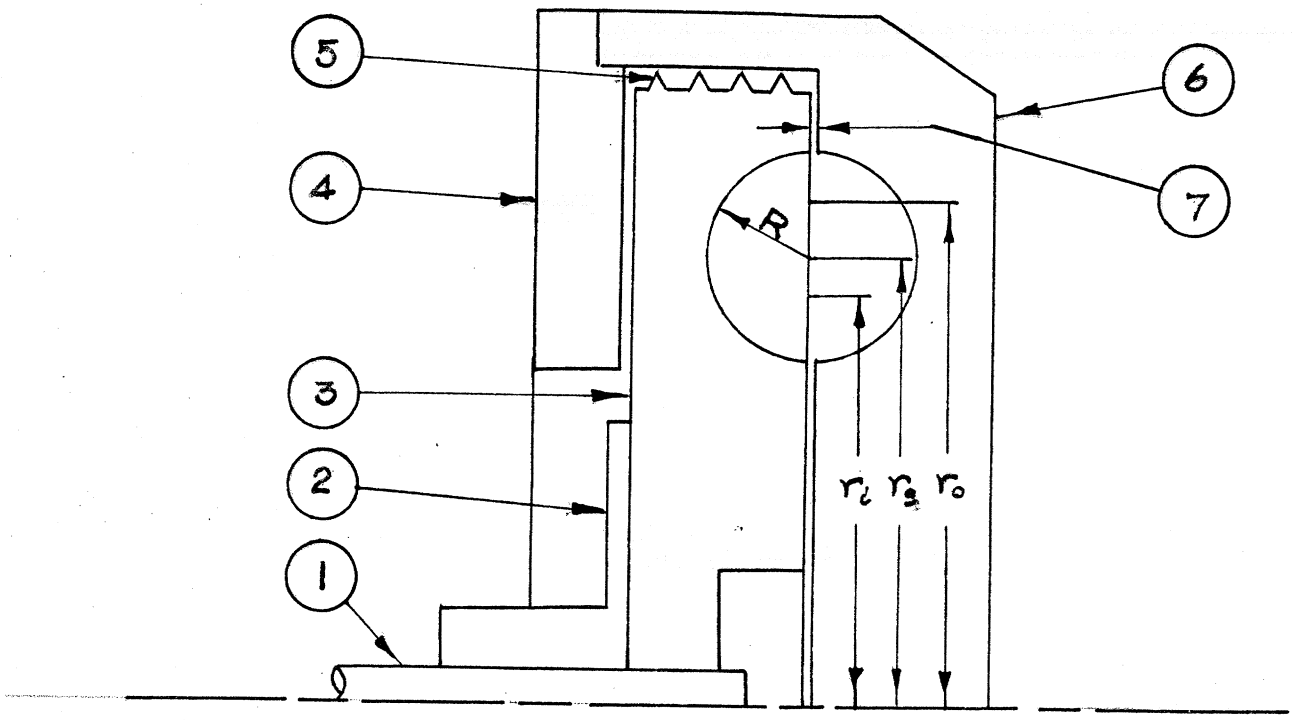

1	IMPELLER SHAFT
2	IMPELLER HUB
3	IMPELLER
4	BACK PUMP SUPPORT PLATE
5	IMPELLER SEALS [CLEARANCE = 0.008 IN.]
6	FRONT COVER OF PUMP
7	CLEARANCE BETWEEN IMPELLER & FRONT COVER
R	RADIUS OF PUMP CHANNEL
r_g	RADIUS TO CENTROID OF CHANNEL AREA
r_i	RADIUS TO MEAN STREAMLINE - Q_c INTO IMPELLER
r_o	RADIUS TO MEAN STREAMLINE - Q_c OUT OF IMPELLER

CROSS SECTION OF EXPERIMENTAL PUMP

FIGURE C

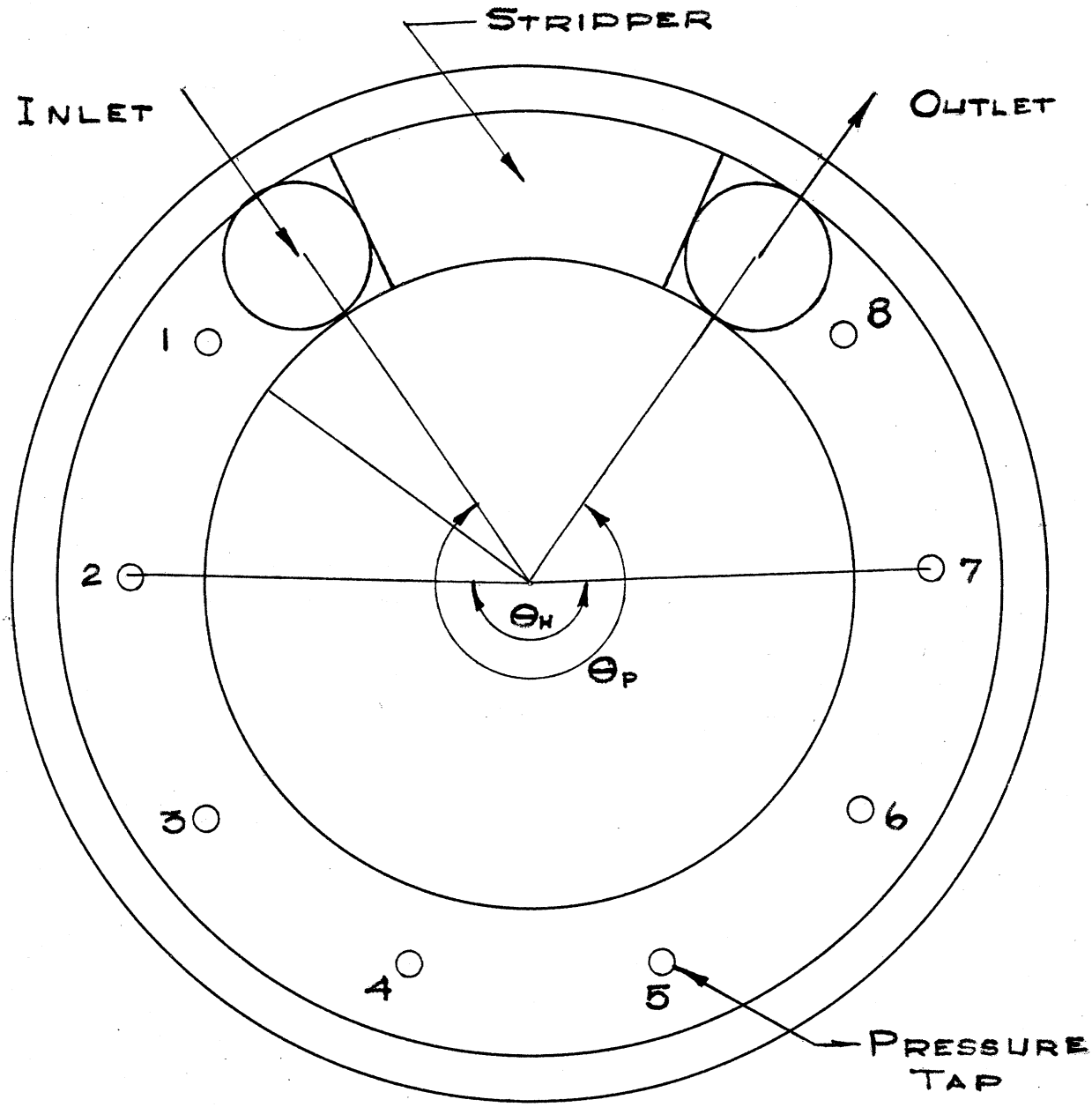

SCHEMATIC DIAGRAM

CHANNEL SECTION

FIGURE D

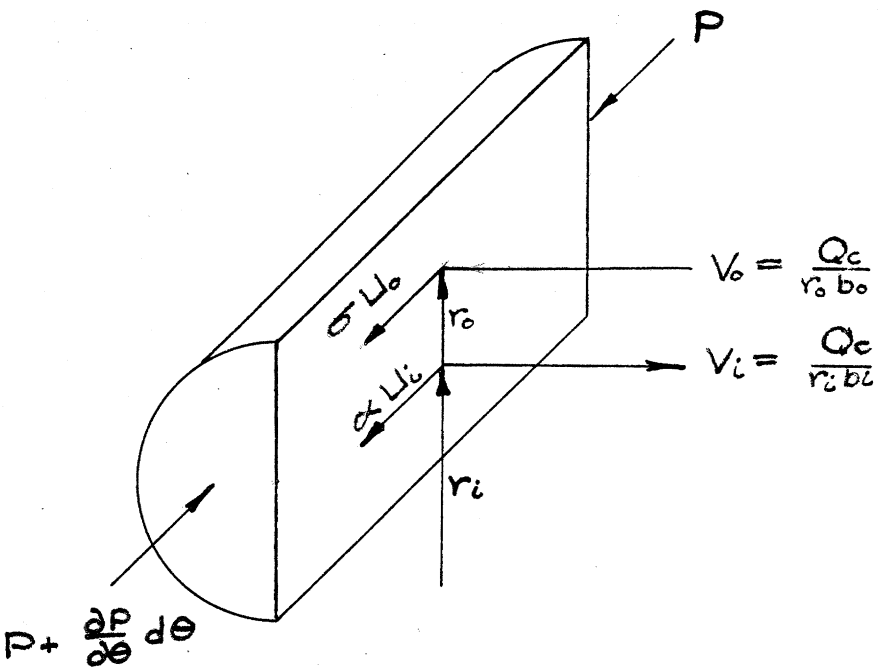

CHANNEL CONTROL VOLUME

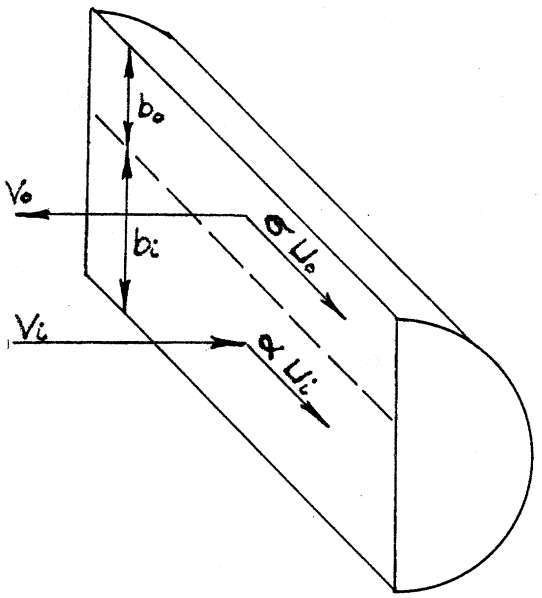

IMPELLER CONTROL VOLUME

CONTROL VOLUMES USED IN THE ANALYSIS

FIGURE E

GRAPH 1

EXPERIMENTAL
INTERNAL PERFORMANCE
[BASED UPON ENTRANCE FLOW]

R = 1 IN. Z = 40 BLADES

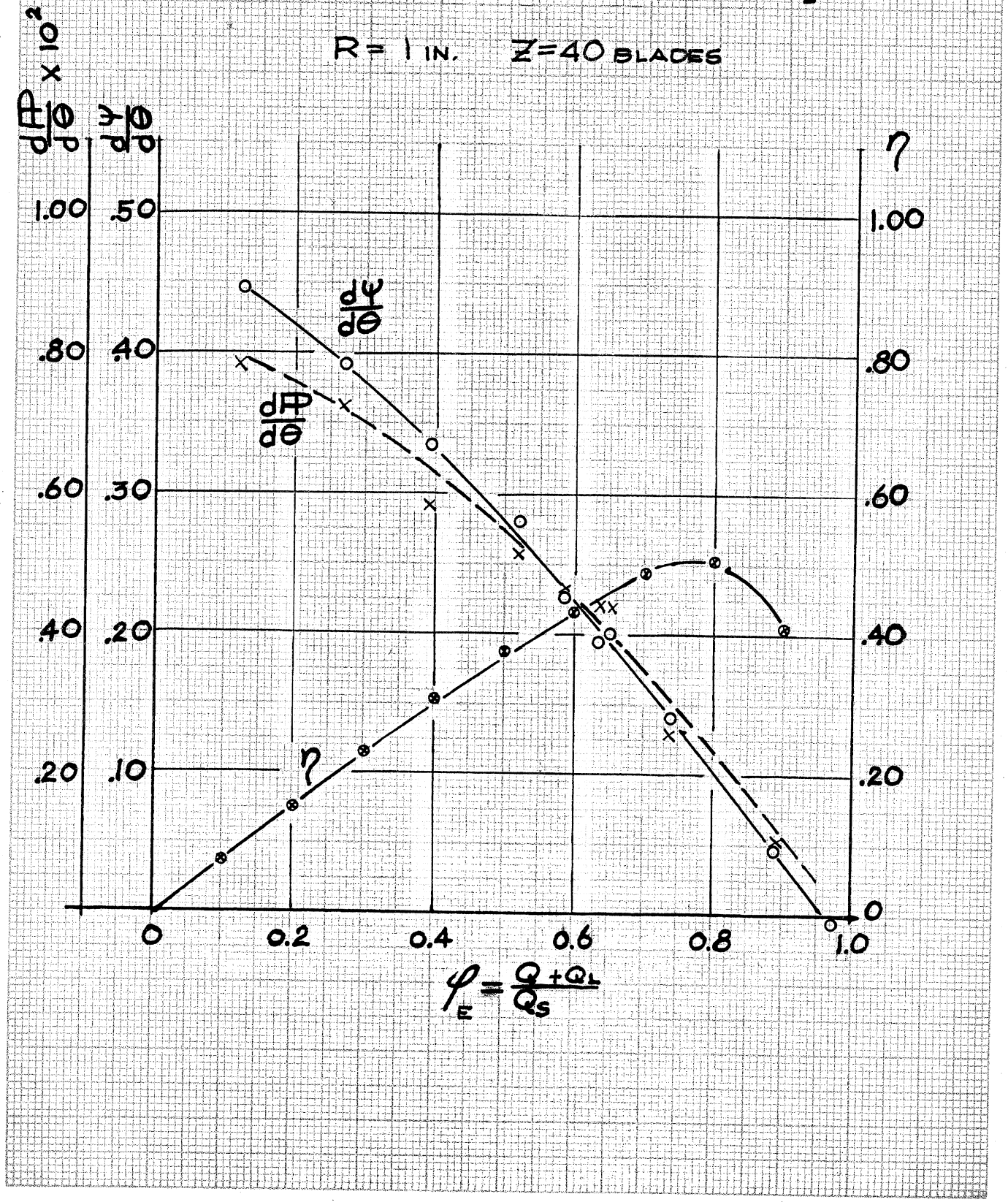

GRAPH 2

EXPERIMENTAL

INTERNAL PERFORMANCE

[BASED UPON ENTRANCE FLOW]

R = 1 INCH Z = 20 BLADES

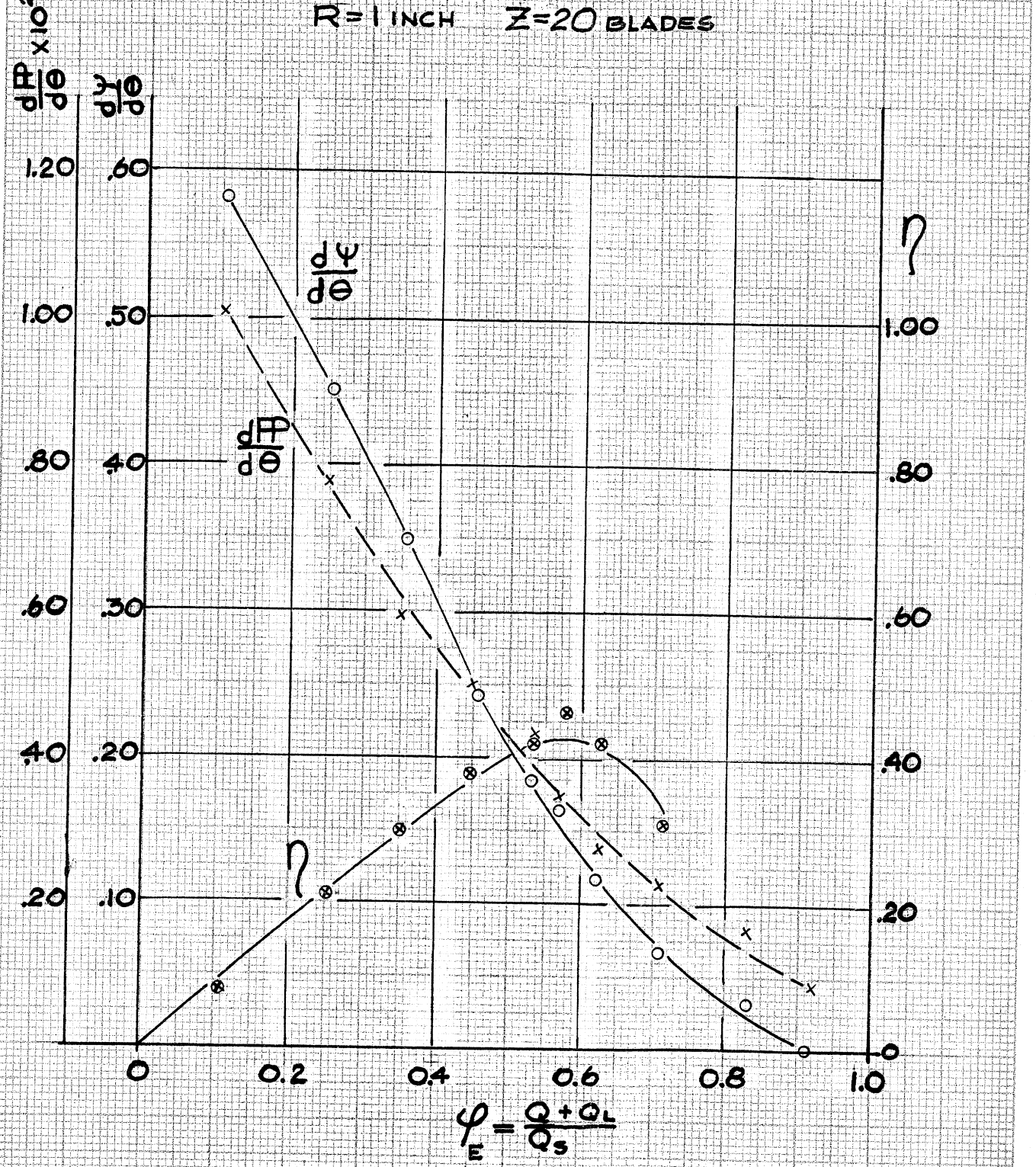

GRAPH 3

EXPERIMENTAL
INTERNAL PERFORMANCE
[BASED UPON ENTRANCE FLOW]
R=0.625 IN. Z=40 BLADES

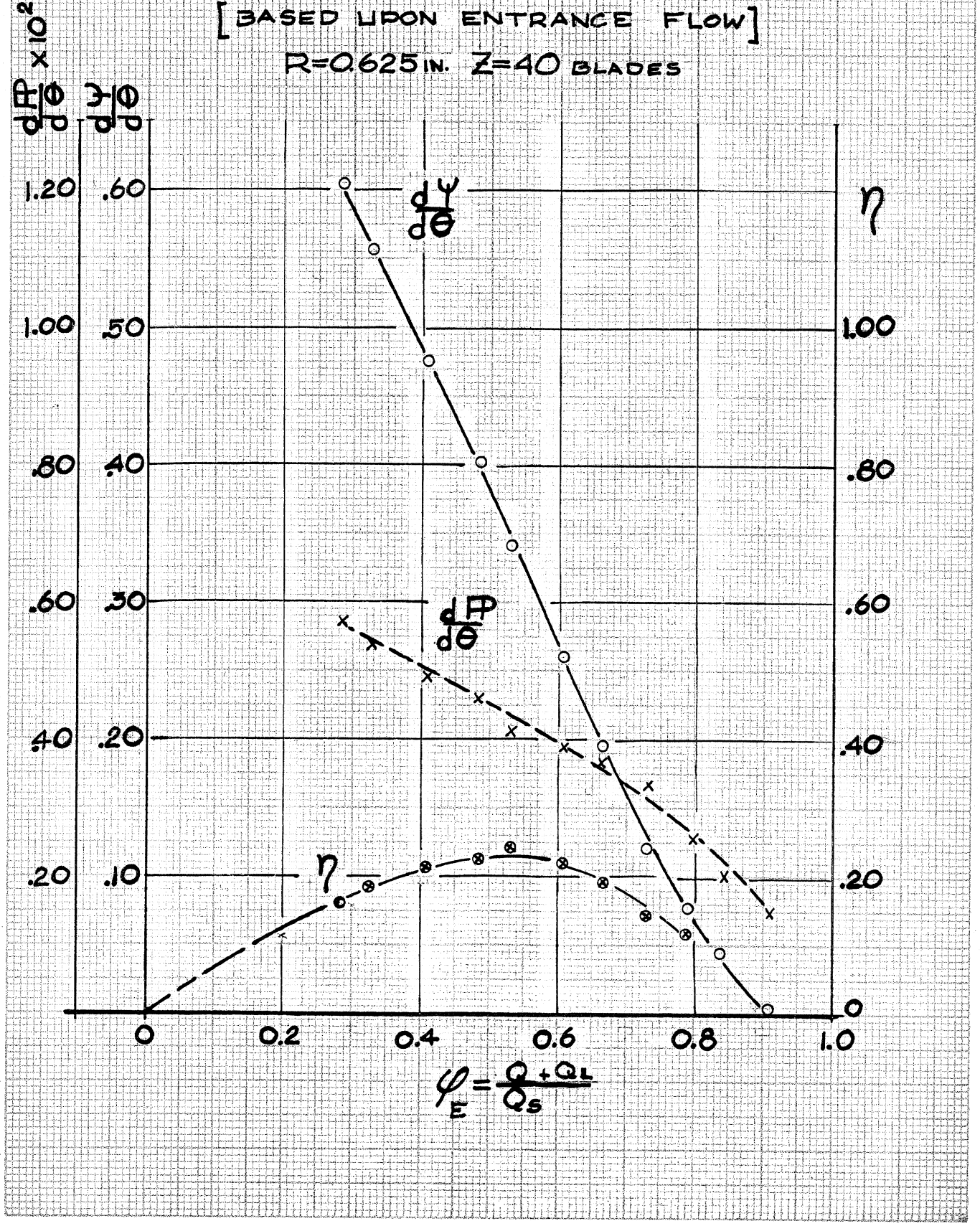

GRAPH 4

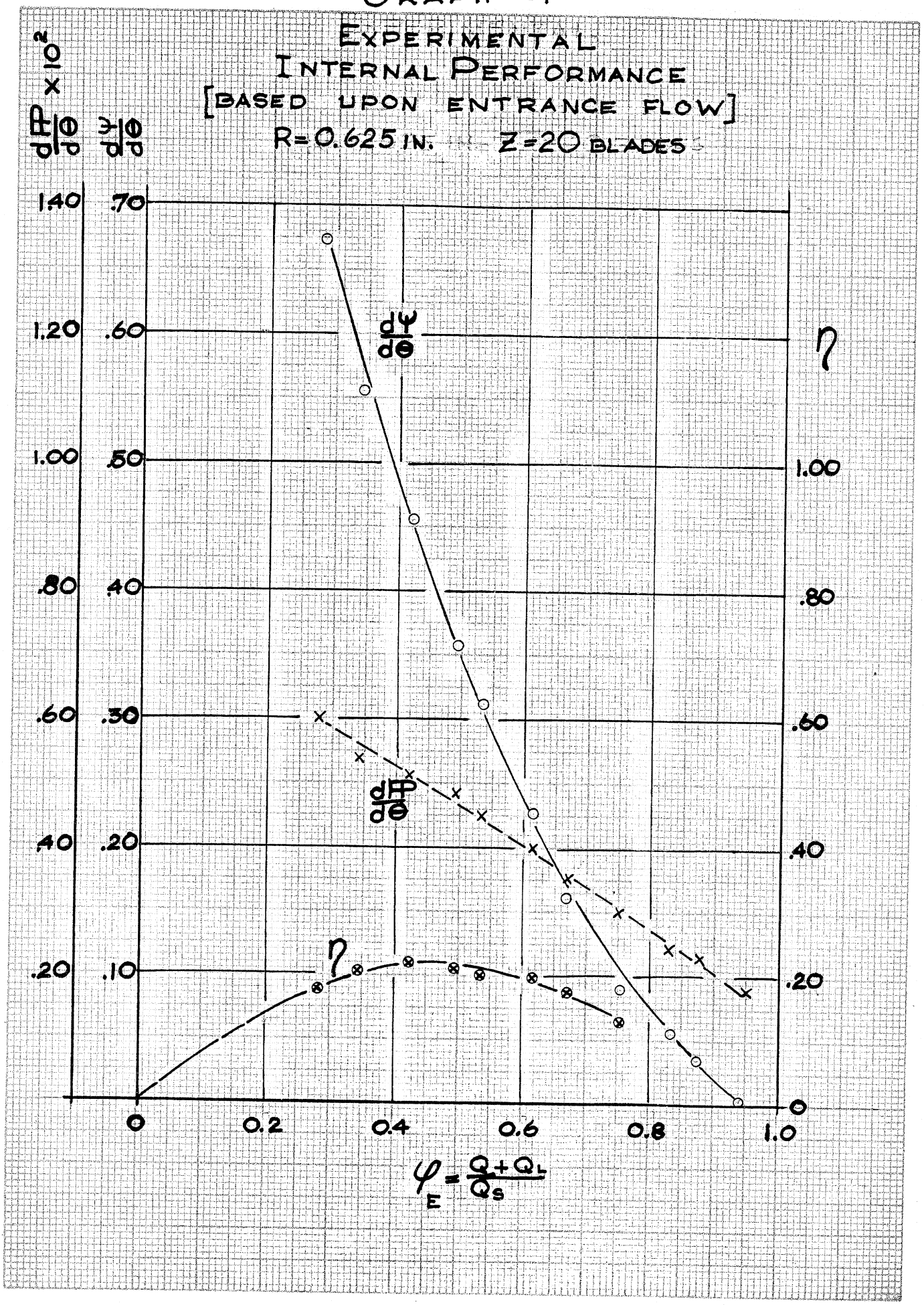

GRAPH 5
INTERNAL PERFORMANCE
BASED UPON DELIVERED FLOW
[CALCULATED FROM EXPERIMENTAL DATA]

R - 1 INCH

Z - 40 BLADES

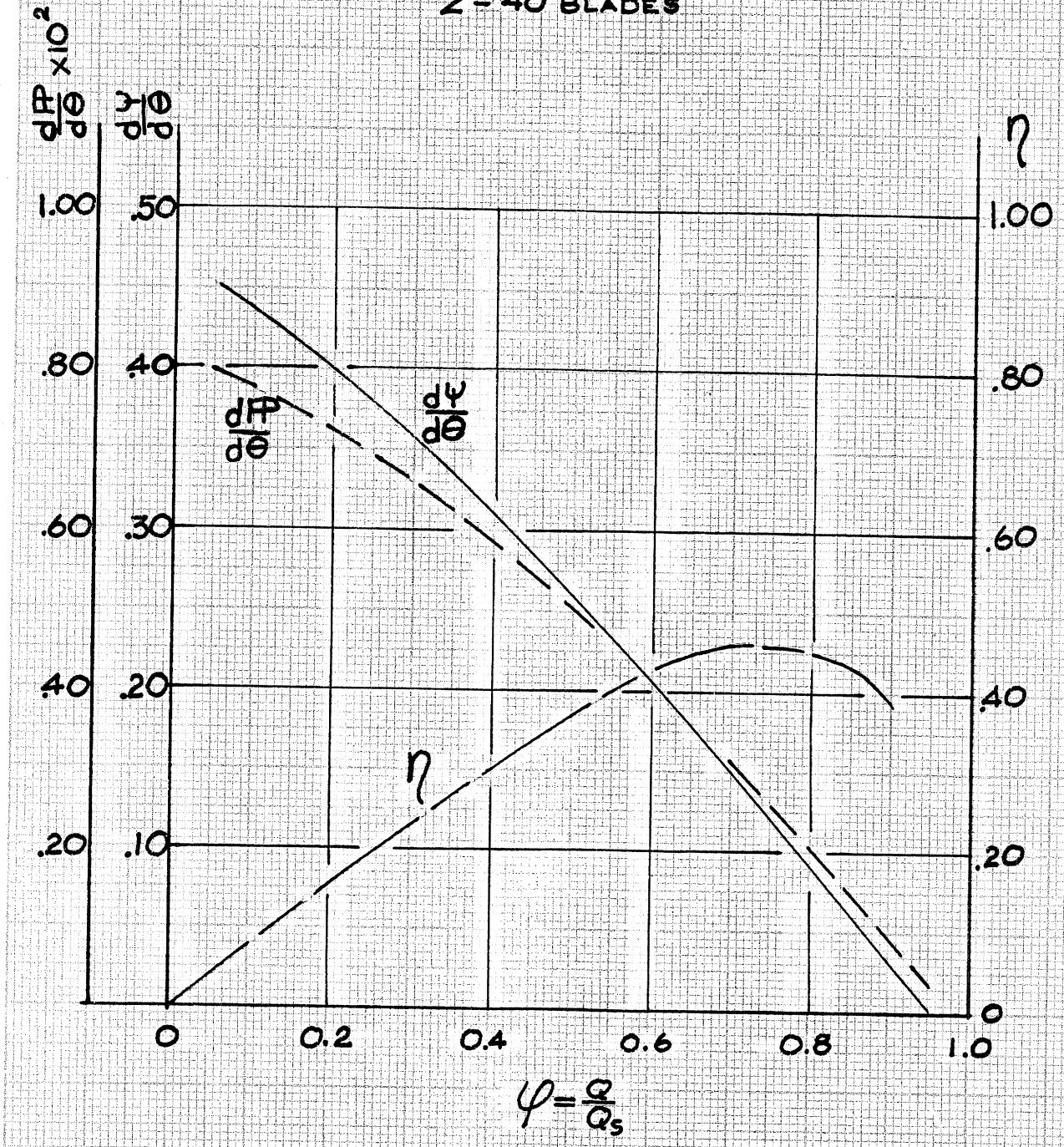

GRAPH 6
INTERNAL PERFORMANCE
BASED UPON DELIVERED FLOW
[CALCULATED FROM EXPERIMENTAL DATA]

R-1 INCH
Z-20 BLADES

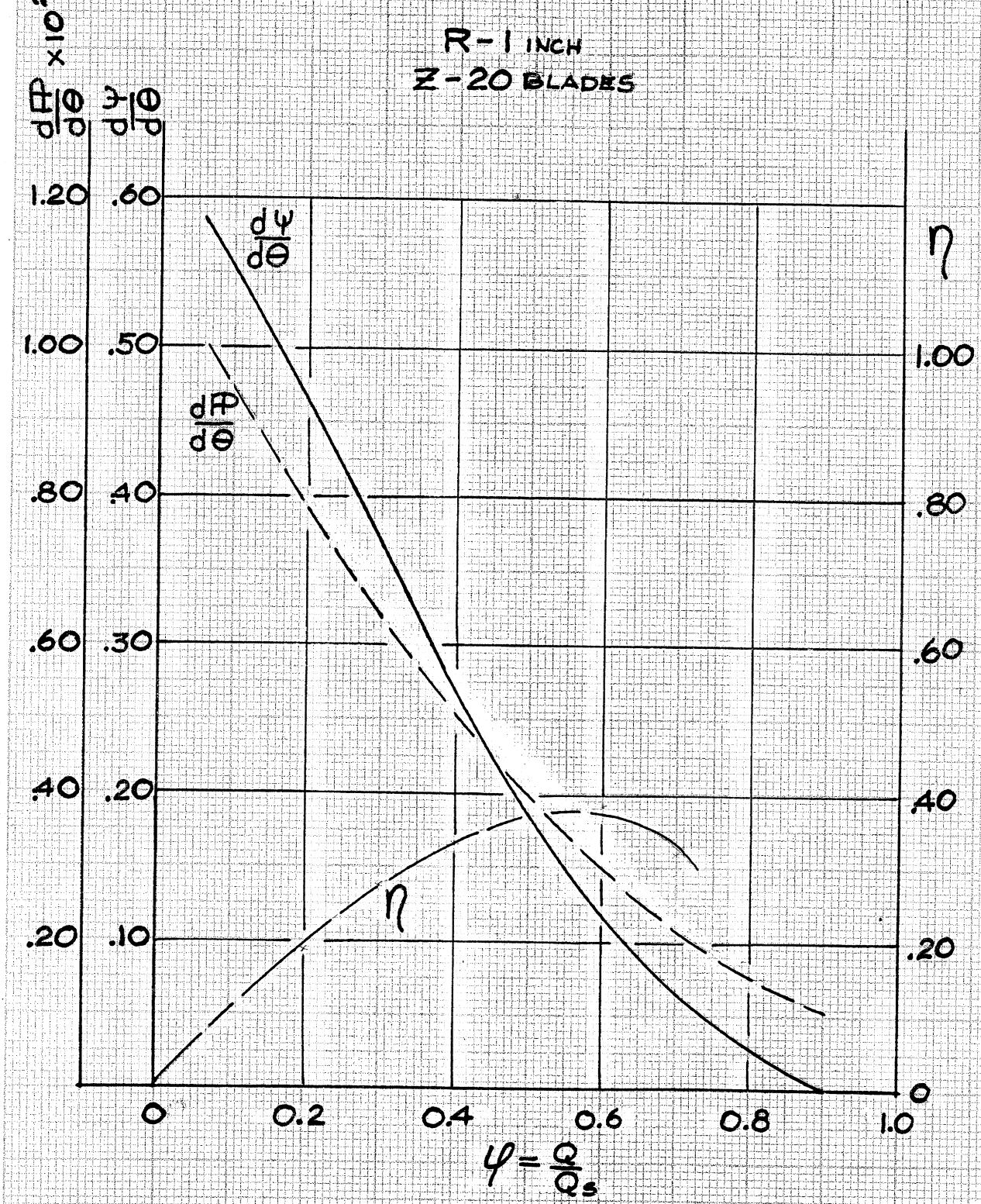

GRAPH 7
INTERNAL PERFORMANCE
BASED UPON DELIVERED FLOW
[CALCULATED FROM EXPERIMENTAL DATA]

R - 0.625 IN.
Z - 40 BLADES

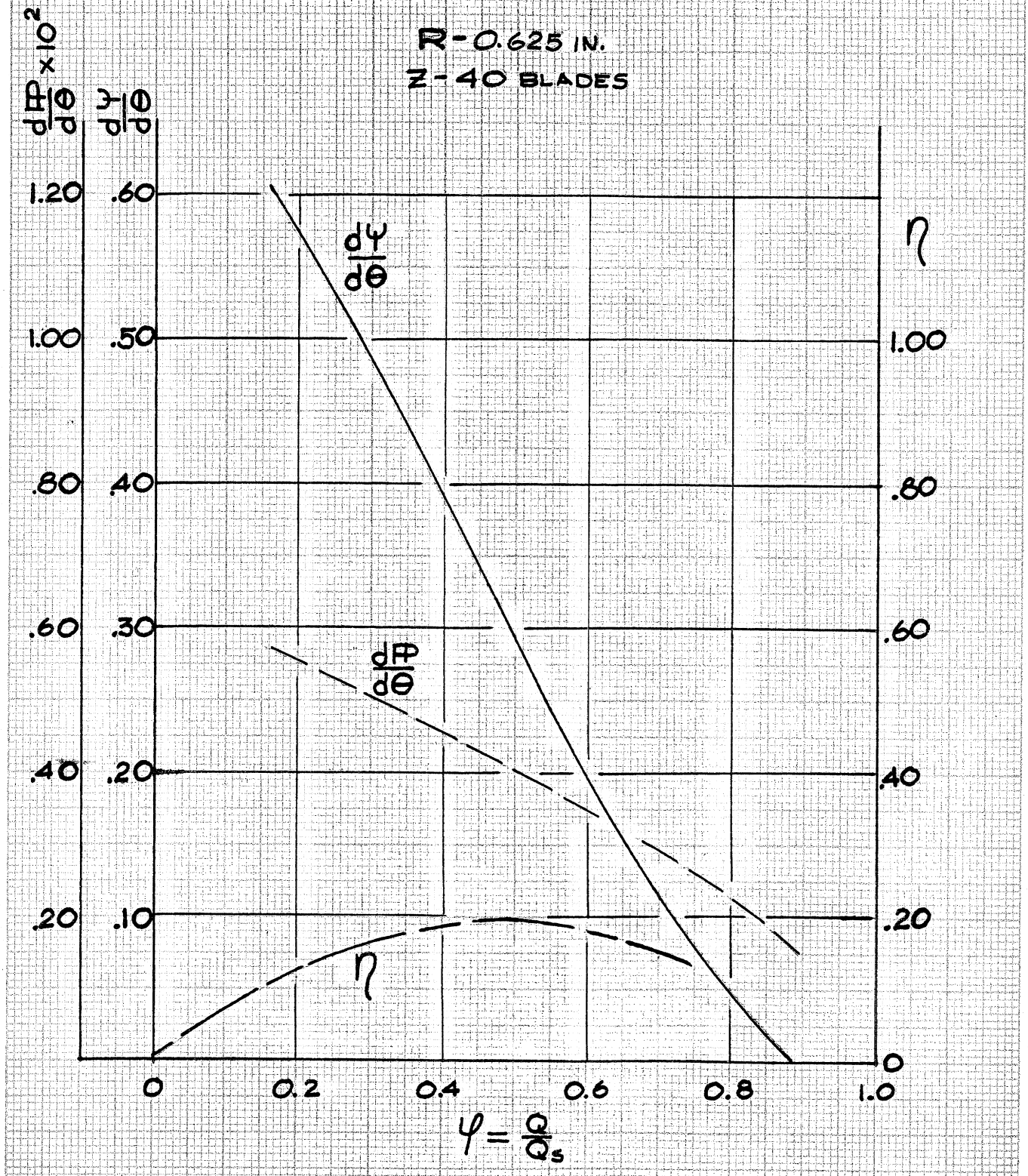

GRAPH 8

INTERNAL PERFORMANCE
BASED UPON DELIVERED FLOW
[CALCULATED FROM EXPERIMENTAL DATA]

R = 0.625 IN. Z = 20 BLADES

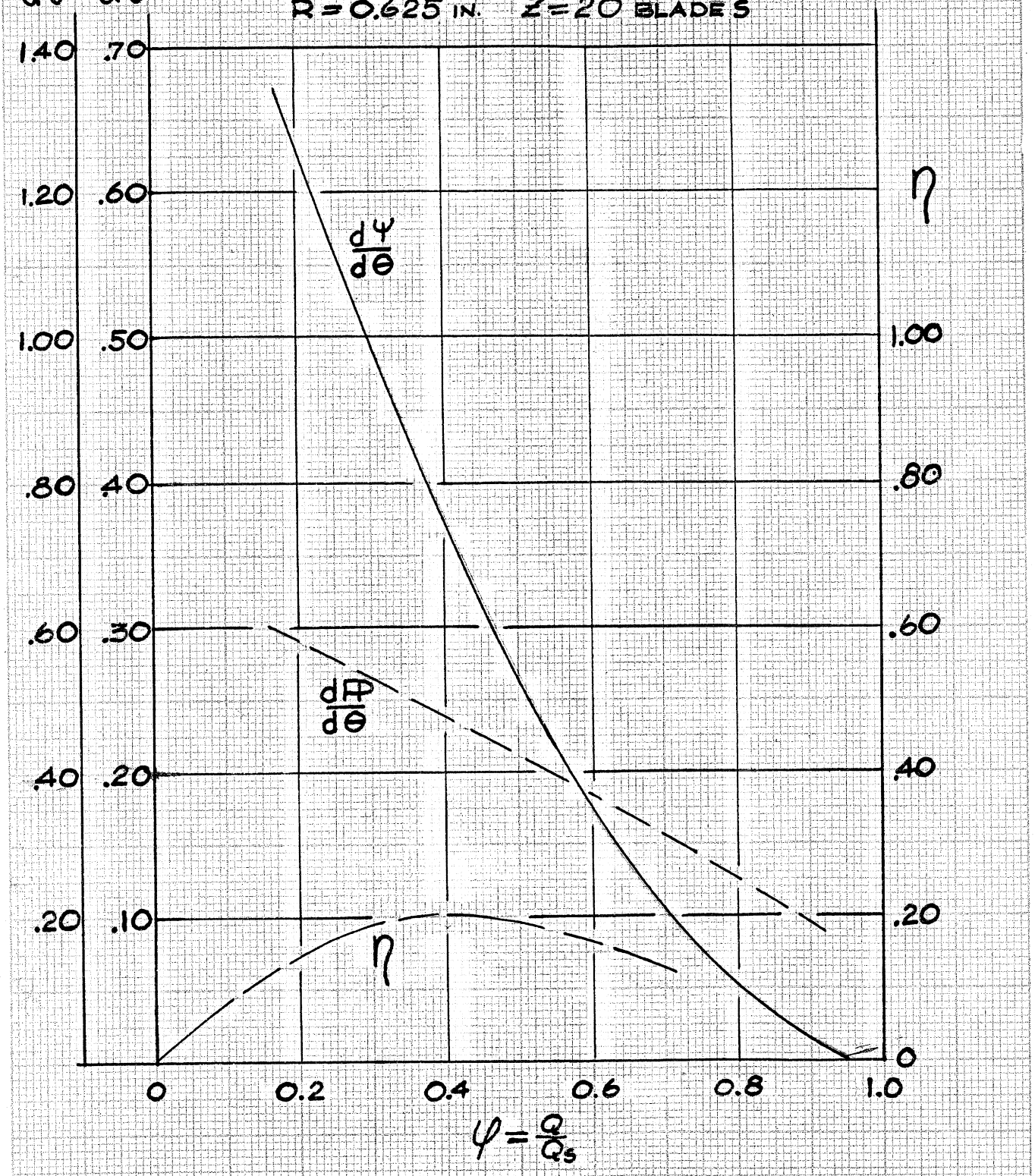

GRAPH 9

THEORETICAL VS EXPERIMENTAL CURVE

R = 1 INCH Z = 40 BLADES

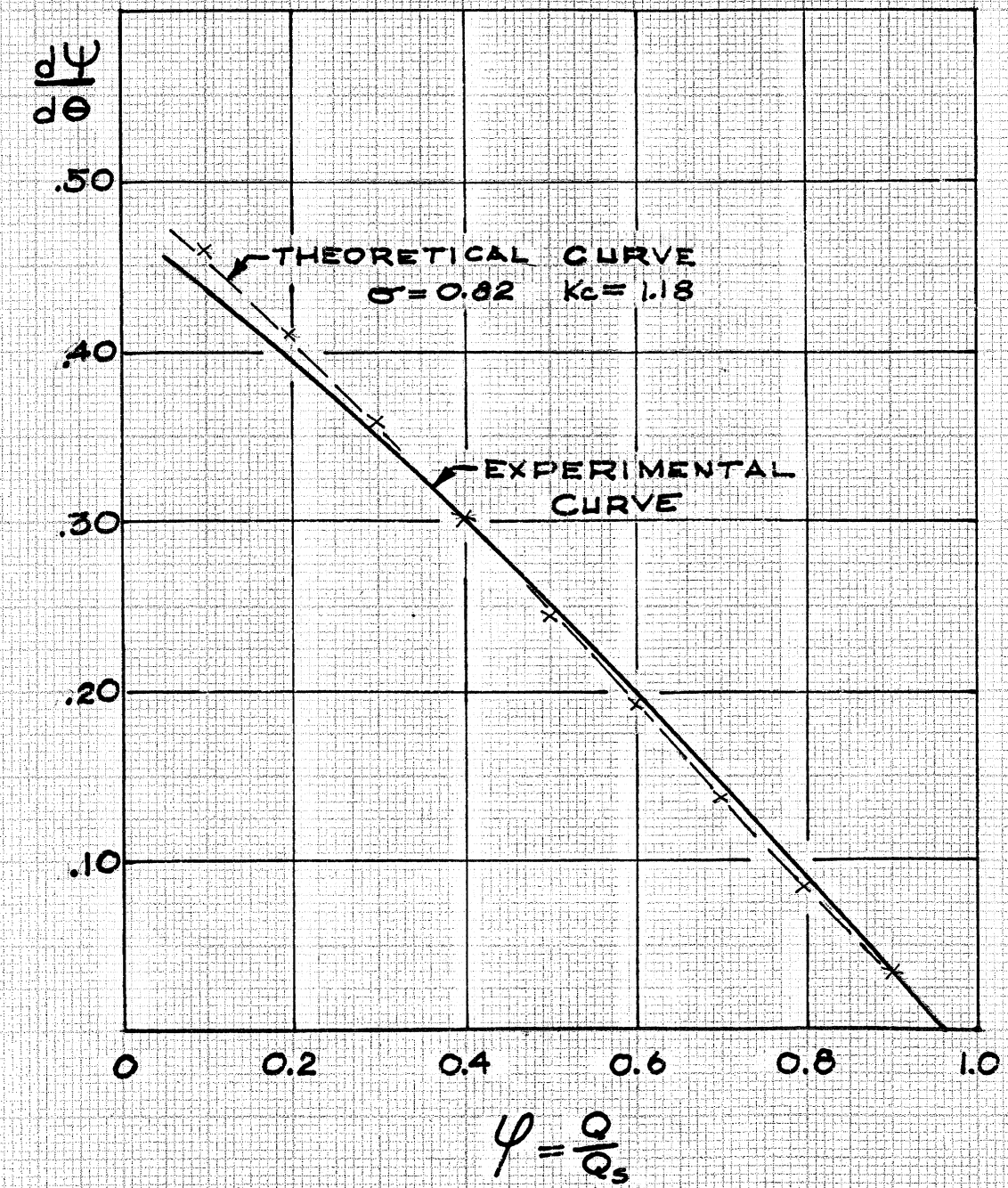

GRAPH 10

THEORETICAL VS EXPERIMENTAL CURVE

R = 1 INCH Z = 20 BLADES

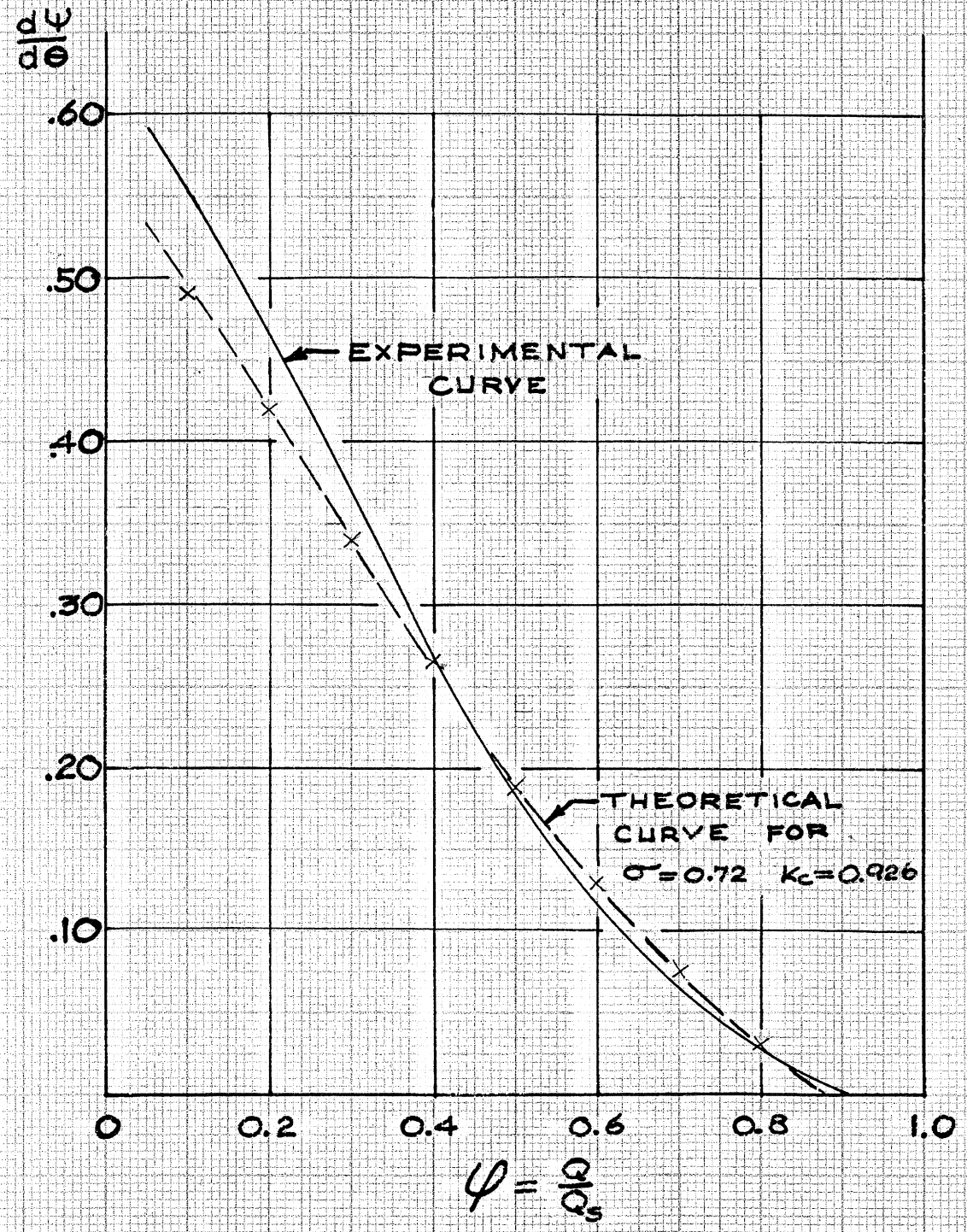

GRAPH 11

THEORETICAL VS EXPERIMENTAL CURVE

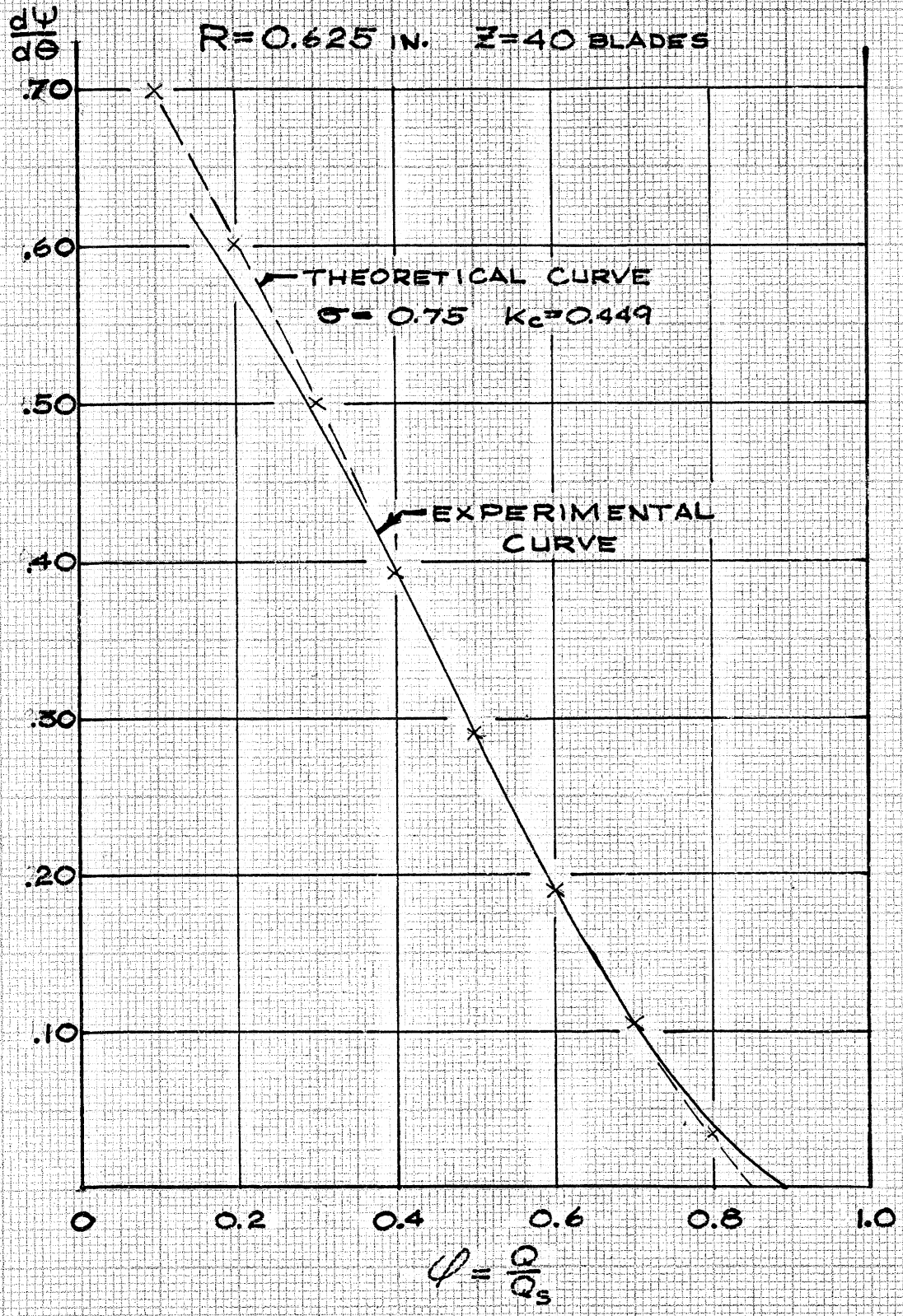

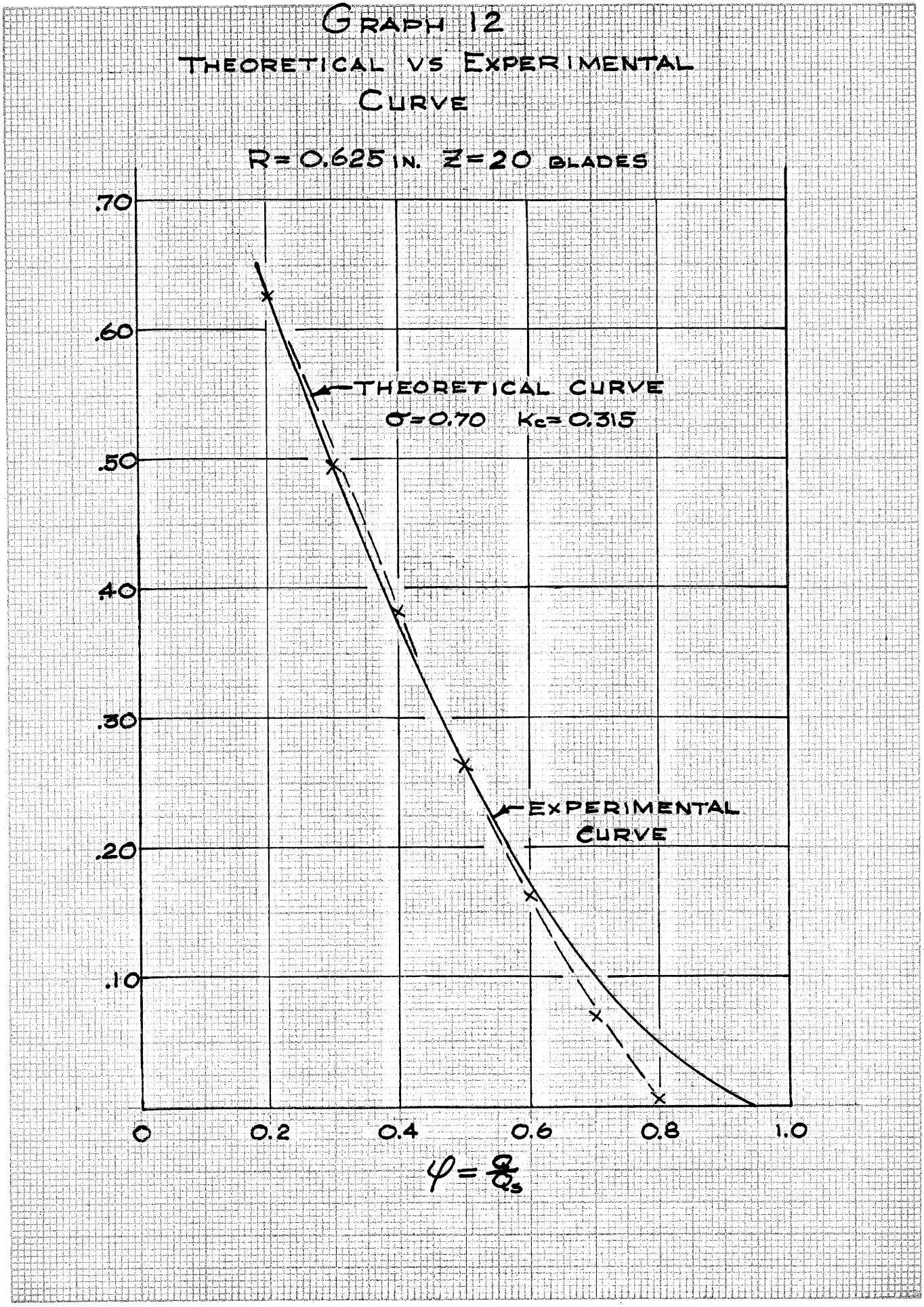
GRAPH 12
THEORETICAL VS EXPERIMENTAL CURVE
R=0.625 IN. Z=20 BLADES
.70
.60
.50
.40
.30
.20
.10
THEORETICAL CURVE
σ=0.70 Kc=0.315
EXPERIMENTAL CURVE
0
0.2
0.4
0.6
0.8
1.0
φ = Q/Qs

APPENDIX

CONSTANTS USED IN THE ANALYSIS

	1	2	3	4
R	1.00	1.00	0.625	0.625
Z	40	20	40	20
A (in^2)	1.57	1.57	0.614	0.614
r_g	3.87	3.87	3.875	3.875
r_o	4.43	4.43	4.213	4.213
r_i	3.432	3.432	3.588	3.588
r_i/r_g	0.886	0.886	0.926	0.926
b_o	0.875	0.875	0.574	0.574
b_i	1.125	1.125	0.676	0.676
c_1	1.10	0.955	0.885	0.827
c_2	0.915	0.854	0.871	0.844
	0.83	0.72	0.75	0.70
K_c	1.18	0.926	0.449	0.315

DIMENSIONLESS THEORETICAL PERFORMANCE EXPRESSIONS

An expression has been derived for the theoretical pressure gradient which is applicable only to the linear region of the pump

$$\frac{dP}{d\theta} = \frac{\rho Q_c}{r_g A}\left(\sigma U_o r_o - \alpha U_i r_i\right) - g H_t \qquad (3)$$

where

$$Q_c = \frac{r_i b_i}{\sqrt{K_c}}\left[\left(\sigma U_o^2 - \alpha U_i^2\right)\left(1 - \frac{Q}{r_g A}\right) - \frac{(1-\alpha)^2 U_i^2}{2}\right]^{\frac{1}{2}} \qquad (6)$$

$$\sigma = \frac{V_t \text{ actual}}{U_o} \quad , \quad \alpha = \frac{V_t \text{ actual}}{U_i}$$

$g H_t$ = tangential flow losses in the impeller

The empirical parameter, α, can be eliminated from the pressure gradient expression by solving the equation of through flow for α and substituting this value into expression 3.

$$\alpha = \frac{1}{U_i}\left[\frac{2Q}{A} - \sigma U_o\right]$$

After substitution and simplification of equations 3, the theoretical pressure gradient can be evaluated by the use of only two parameters (σ & K_c) which must be determined empirically. The modified equation 3 is then non-dimensionalized for ease in calculations.

$$\frac{d\Psi}{d\theta} = \frac{1}{2}\,\frac{r_i}{r_g}\,\frac{Q_c}{Q_s}\left(C_1 - \phi\right)$$

where $$\frac{Q_c}{Q_s} = \frac{r_i b_i}{A}\sqrt{\frac{2}{K_c}}\sqrt{\frac{r_o}{r_i}}\sqrt{(C_1-\phi)(1-\phi) - \frac{r_g}{r_i}(C_2-\phi)^2}$$

$$C_1 = 2\frac{r_o^2}{r_i r_g}\left(1 + \frac{r_i}{r_o}\right)\sigma$$

$$C_2 = \frac{r_i}{2 r_g}\left(1 + \frac{r_o}{r_i}\sigma\right)$$

LEAKAGE ANALYSIS

There are several sources of leakage within the regenerative pump:

a. Leakage occurs across the impeller seals which is proportional to the pressure difference across the impeller at any point.

b. A portion of the fluid within the channel passes between the impeller and the cover at the stripper region. Attempts were made to minimize this source of leakage by keeping the clearance between the impeller and cover at 0.005 inches throughout all tests.

Previous work has shown that the major source of leakage occurs through the impeller seals. The leakage correction factor as derived by DeWitt (1) has been applied to the experimental curves and is shown in Graphs 5, 6, 7, and 8.

The following is a summary of the seal leakage:

$$\varphi_{Loc} = \varphi_M - \int_0^{\theta} \varphi_L \, d\theta$$

where φ_{Loc} flow at any point considered

φ_M measured flow at inlet

φ_L leakage flow/radian

θ angle from the inlet

the leakage flow/radian, φ_L , is assumed to be proportional to the square root at the pressure coefficient at any point.

$$\varphi_L = k\sqrt{\psi}$$

The expression for the leakage flow was then integrated in order to determine a mean value for the leakage flow. The results of this integration are shown below.

$$\Phi_L = \varphi_L' \sqrt{\psi/\psi'}$$

where $\varphi_L' = \frac{2}{5} \varphi_M'$

φ_M' is measured at $\varphi_{exit} = 0$

ψ' shut off head

BIBLIOGRAPHY

(1) DeWitt, D. P. — "Rational Design and Development of the Regenerative Pump" M. S. Thesis, M.I.T., January, 1957

(2) Santalo, M. A. — "Experimental Investigation of the Variables Affecting Regenerative Pump Performance" M. S. Thesis, M.I.T., June, 1954

(3) Wilson, Santalo and Oelrich — "A Theory of the Fluid Dynamic Mechanism of Regenerative Pumps" Transactions of the ASME, November 1955, Volume 77, No. 8